ChemPubSoc Europe

DOI: 10.1002/cctc.201402096

Titania-Supported Gold Nanoparticles as Efficient Catalysts for the Oxidation of Cellobiose to Organic Acids in Aqueous Medium

Prince N. Amaniampong,[a, b] Kaixin Li,[a] Xinli Jia,[a] Bo Wang,[b] Armando Borgna,*[b] and Yanhui Yang*[a]

Titania-supported gold nanoparticles were prepared by using the deposition–precipitation method, followed by reduction under a hydrogen flow. The catalytic activity of these as-prepared catalysts was explored in the oxidation of cellobiose to gluconic acid with molecular oxygen, and the properties of these catalysts were examined by using XRD, TEM, temperature-programmed desorption of NH_3, energy-dispersive X-ray spectroscopy, UV/Vis, and X-ray photoemission spectroscopy (XPS). The catalyst sample reduced at high temperature demonstrated an excellent catalytic activity in the oxidation of cellobiose. The characterization results revealed the strong metal–support interaction between the gold nanoparticles and titania support. Hydrogen reduction at higher temperatures (usually $>600\,^{\circ}C$) plays a vital role in affording a unique interface between gold nanoparticles and titania support surfaces, which thus improves the catalytic activity of gold/titania by fine-tuning both the electronic and structural properties of the gold nanoparticles and titania support.

Introduction

It has been extensively discussed that biomass conversion substantially contributes to the sustainable development of our society. The production of fuels and chemicals from renewable biomass has a significant effect on decreasing carbon dioxide emission from fossil fuel combustion because the released carbon dioxide can be consumed during the subsequent regrowth of biomass. Among various biomass sources, cellulose is a promising candidate because it is abundant in nature, forms 40–50% of biomass composition, and also does not compete with food. Nonetheless, there are several technical issues that hamper the use of cellulose to produce energy fuels and platform chemicals.[1]

The catalytic hydrotreating of cellulose has been investigated to produce a wide range of sugars and polyols such as glucose, ethylene glycol, propylene glycol, and sorbitol, which are key raw materials or intermediates in petrochemical, pharmaceutical, food, and cosmetic industries as well as considered as a new generation of green energy platform.[2,3] In addition to the cellulose hydrotreating process, the selective oxidation of cellulose attracted growing attention because it yields important biomass-derived chemicals such as gluconic acid and its derivatives, which are widely used in pharmaceutical applications and in the food industry as water-soluble cleansers and additives.[4] Furthermore, air can be used as the oxidant, which significantly reduces the processing cost as compared to hydrotreating processes.

For the direct conversion of cellulose into organic acids under an oxidative atmosphere, bifunctional or multifunctional catalysts are often required.[5] These bifunctional catalysts not only perform cascade or multistep reactions in one pot but also may increase overall efficiency and product selectivity. Many bifunctional catalysts have been tested for the oxidative conversion of glucose to organic acids. Recent studies reported that gold catalysts, especially supported gold nanoparticles, can catalyze the oxidation of glucose to gluconic acid.[6]

Wang and co-workers examined the conversion of cellobiose (a representative compound of cellulose) over gold nanoparticles supported on various supports.[7] They found that the carbon nanotube (CNT) was the best support for the formation of gluconic acid in aqueous medium, with a cellobiose conversion of 91% and a gluconic acid selectivity of 60% at a reaction time of 3 h. This group further investigated the conversion of cellobiose over CNT-supported palladium, platinum, rhodium, copper, and silver catalysts. The best results were obtained with the platinum/CNT catalyst (cellobiose conversion of 53% and gluconic acid selectivity of 23%).[7] An et al. converted cellobiose to gluconic acid over gold nanoparticles loaded on Al_2O_3, HZSM-5, $C_{S1.2}H_{1.8}PW_{12}O_{40}$, and $C_{S1.7}H_{1.3}PW_{12}O_{40}$. A cellobiose conversion of 92% and a gluconic acid selectivity of 71% were achieved over the gold nanoparticles loaded on $C_{S1.7}H_{1.3}PW_{12}O_{40}$, which was the most efficient catalyst for cellobiose conversion.[8]

These results revealed that the nature of the support played an important role in cellobiose conversion. In addition, other

[a] P. N. Amaniampong, Dr. K. Li, Dr. X. Jia, Dr. Y. Yang
School of Chemical and Biomedical Engineering
Nanyang Technological University
62 Nanyang Drive, 637459 (Singapore)
E-mail: Armando_Borgna@ices.a-star.edu.sg
yhyang@ntu.edu.sg

[b] P. N. Amaniampong, Dr. B. Wang, Dr. A. Borgna
Heterogeneous Catalysis Division
Institute of Chemical and Engineering Sciences
A*STAR (Agency for Science, Technology and Research)
1 Pesek Road, Jurong Island, 627833 (Singapore)

parameters such as reaction temperature, reaction time, pressure, and solvent may affect the conversion of cellobiose to organic acids, although the effects of these parameters have not been studied systematically. Herein, we report the work using gold nanoparticles supported on TiO_2 for the oxidation of cellobiose. The effect of the reduction temperature of catalyst pretreatment was investigated. High-temperature reduction under a hydrogen atmosphere was generally considered to agglomerate the gold nanoparticles; surprisingly, the catalyst prereduced at high temperature herein afforded excellent catalytic activity and selectivity toward the desired organic acid. Furthermore, a kinetic study was performed and the reaction parameters such as temperature, pressure, and solvent were optimized.

Results and Discussion

Catalytic activity of Au nanoparticles loaded on different supports

The catalytic oxidation of cellobiose over Au/TiO_2, Au/CNT, and Au/zeolite HY catalysts was performed under the same reaction conditions, and the results are presented in Figure 1. Although both CNT and zeolite HY-supported Au nanoparticles could convert cellobiose to gluconic acid with a reasonably good selectivity, the catalytic results clearly indicated that TiO_2 outperformed other supports and the Au nanoparticles supported on TiO_2 demonstrated the highest conversion and selectivity toward gluconic acid.

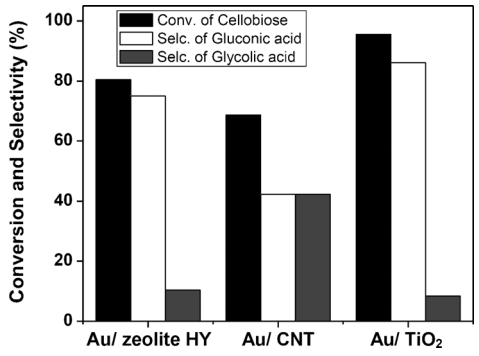

Figure 1. Au catalyst loaded on zeolite HY, CNT, and TiO_2 supports. Reaction conditions: 0.300 mmol of cellobiose, 20 mL of H_2O, 0.050 g of the catalyst, $P = 0.5$ MPa O_2, $t = 3$ h (other reaction products include fructose, glycolic acid, fructose, sorbitol, and ethylene glycol).

To understand the superior performance of Au on the TiO_2 support, cellobiose conversion using TiO_2 in the absence of Au nanoparticles was performed. A high cellobiose conversion (95.3%) was obtained at 145 °C, and the primary product was glucose (selectivity of 91.2%) without gluconic acid. Compared with the literature results, a cellobiose conversion of 27% was reported when the CNT alone was used in cellobiose conversion at 148 °C, glucose was the main product (selectivity 80%) as reported by Deng et al.[10] These results suggested that the hydrolysis of cellobiose to glucose can be readily performed with supports, and TiO_2 outperformed other supports for cellobiose hydrolysis, which can be accounted for the high activity in the one-pot conversion of cellobiose. If the support was loaded with Au nanoparticles, the formation of gluconic acid was observed, which suggested that the Au nanoparticles were the primary catalytic sites for oxidation. The acid-catalyzed hydrolysis of cellobiose to glucose with the TiO_2 support followed by the oxidation of glucose to gluconic acid catalyzed by the Au nanoparticles reveals the bifunctional nature of the as-prepared Au/TiO_2 catalyst.

Furthermore, the Au/TiO_2 catalyst was reduced at different temperatures under a H_2 flow and then tested in the oxidative conversion of cellobiose. As shown in Figure 2, the reduction temperature of the as-prepared catalyst affected its catalytic activity in converting cellobiose to gluconic acid. An increase in the reduction temperature from 400 to 700 °C increased both the conversion of cellobiose and selectivity toward gluconic acid from 88.7 and 65.0 to 95.5 and 86.0%, respectively.

The acid–base properties of different supports may not play a key role with respect to the selectivity toward gluconic acid

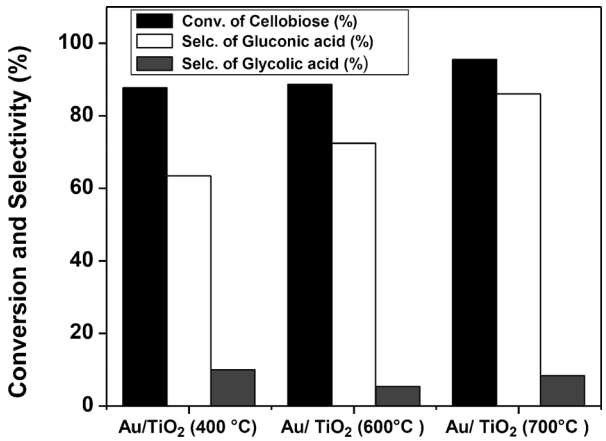

Figure 2. Au/TiO_2 catalyst reduced at different temperatures (400, 600, and 700 °C) for cellobiose oxidation. Reaction conditions: 0.300 mmol of cellobiose, 20 mL of H_2O, 0.050 g of the catalyst, $P = 0.5$ MPa O_2, $t = 3$ h (other reaction products include fructose, glycolic acid, sorbitol, and ethylene glycol).

because the hydrolysis of cellobiose was not the limiting step.[11] Hence, oxidation was considered as the key step for high selectivity toward gluconic acid in one-pot oxidative conversion of cellobiose to gluconic acid. In view of this, fine-tuning the properties of Au nanoparticles, for example, particle size, electronic structure, and the specific interaction between Au nanoparticles and the support, can control the catalyst selectivity toward gluconic acid. If the Au catalyst possessed a high activity for glucose oxidation, then the glucose produced via cellobiose hydrolysis (step 1) in the overall reaction mechanism should be readily converted to gluconic acid (step 2), which results in high selectivity. Otherwise, because glucose is multifunctional in nature, it can be substantially decomposed into complex degradation products or the formed gluconic acid may suffer further hydrogenolysis to yield polyols during the reaction, which results in extremely low selectivity.

Characterization of Au/TiO_2 catalysts reduced at different temperatures

Temperature-programmed desorption of NH_3 (NH_3-TPD) characterization was performed to evaluate the acid strength of the catalyst sample. The strength of acid sites on the supported TiO_2 catalyst is presented in Figure 3. Catalytic activities are

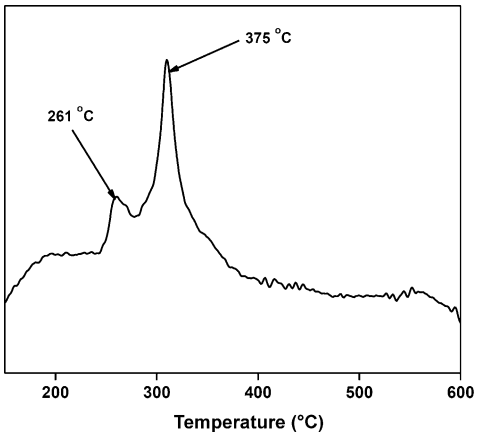

Figure 3. NH_3–TPD of the Au/TiO_2 sample.

correlated with the acid strength of a catalyst. Notably, the strong Lewis acid center in the TiO_2 catalyst, as illustrated in Figure 3, is responsible for the hydrolysis of cellobiose to glucose and the cellobiose conversion depends on the acid strength of the catalyst support. The peaks at the high and low temperatures can be attributed to the desorption of NH_3 from the strong and weak acid sites, respectively. The high-temperature desorption NH_3 was ascribed to the desorption of coordinated NH_3-bound Lewis acid sites.[8] The peak at 261 °C was attributed to the adsorption of NH_3 on weak Brønsted acid sites of the TiO_2 lattice, whereas the strong and conspicuous peak at 375 °C was attributed to the desorption of NH_3 on the strong Lewis acid sites of TiO_2. The latter acidity was the main acidity that was responsible for cellobiose hydrolysis. The total acidity estimated from the analysis of NH_3-TPD was 354.54 $\mu mol\,g^{-1}$, which was comparable to the acid strength of TiO_2 estimated by Yang et al. (362 $\mu mol\,g^{-1}$, with a BET surface area of 79 $m^2\,g^{-1}$).[12]

The as-prepared TiO_2-supported Au nanoparticles were reduced under a H_2 flow at different temperatures and then characterized by applying various characterization techniques. Energy-dispersive X-ray spectroscopy (EDX) analysis revealed the existence of Au and Ti, which indicated that Au nanoparticles were deposited on TiO_2 surfaces. The Au loading determined from X-ray fluorescence (XRF) analysis (1.1 wt%) was consistent with the predetermined value of Au loading during the catalyst synthesis. After cellobiose oxidation, the catalyst was collected and dried. The XRF analysis was performed on the recycled catalyst and the metal loading of 1.0 wt% was obtained, which indicates that no significant leaching occurred and the Au/TiO_2 catalyst can be recycled. For brevity, the EDX image was not shown.

The Au nanoparticles observed by using TEM are characterized with the semispherical shape practically without well-detectable crystallographic planes. The Au nanoparticles were homogeneously dispersed on the TiO_2 support. The distribution of Au particles for the samples reduced at 400, 600, and 700 °C and the spent Au/TiO_2 catalysts (reduced at 700 °C) are presented in Figure 4. The particle size depended on the nature of the catalyst pretreatment; smaller Au particles were detected for the samples reduced at 400 and 600 °C (particle sizes centered at 4–5 and 6–8 nm, respectively) than for the samples reduced at 700 °C (particles sizes centered at 10–12 nm). This result was in agreement with the results reported by Tsubota

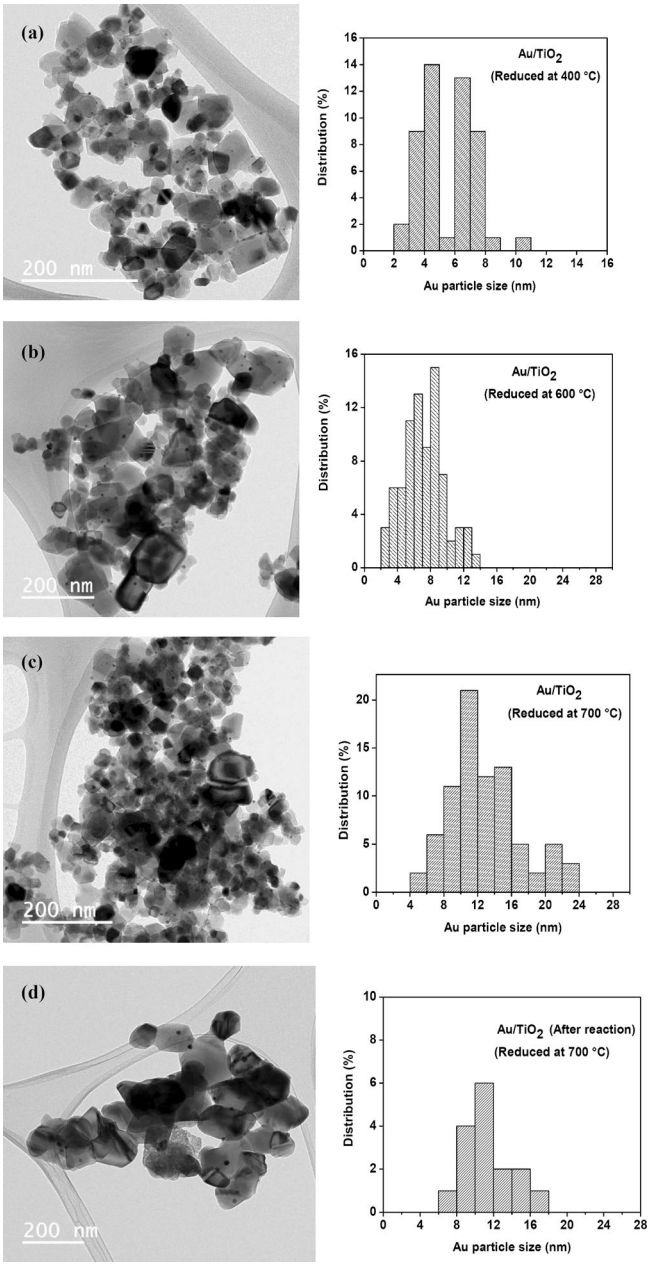

Figure 4. TEM images and particle size distribution of a) 1 wt% Au/TiO_2 reduced at 400 °C, b) 1 wt% Au/TiO_2 reduced at 600 °C, c) 1 wt% Au/TiO_2 reduced at 700 °C, and d) Au/TiO_2 (after the reaction).

et al.[13] Hydrogen atmosphere and high temperature induced the migration of metal clusters, which was evidently shown in the TEM image of the sample reduced at 700 °C as having a larger particle size than the sample reduced at 600 °C. The TEM image of the spent sample (reduced at 700 °C) showed Au nanoparticles centered at 11–12 nm, which indicated no significant particle size changes during the oxidation reaction.

The phase identification of the fresh and spent Au/TiO_2 catalysts was performed by using XRD (Figure 5). The XRD patterns

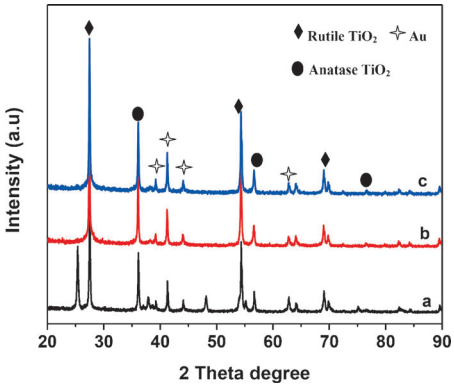

Figure 5. XRD patterns of a) Au/TiO_2 reduced at 600 °C, b) Au/TiO_2 reduced at 700 °C, and c) spent Au/TiO_2 catalyst reduced at 700 °C.

demonstrate strong diffraction peaks at 25, 27.54, 54.29, 70, and 75°, which reveal the mixture of rutile and anatase phases of TiO_2 supports. The diffraction peaks at $2\theta = 36.29$, 41.09, and 64.19° are attributed to the (111), (200), and (220) facets of its face-centered cubic Au metal structure, respectively. The Au particle sizes calculated from XRD data by using the Scherrer method was found to be in conformity with the particle sizes observed with TEM analysis. The XRD pattern of the spent Au/TiO_2 catalyst (reduced at 700 °C) is similar to the XRD pattern of the fresh Au/TiO_2 catalyst before the catalytic reaction, which suggests that Au nanoparticles supported on TiO_2 after reduction at 700 °C were stable during the oxidative conversion of cellobiose.

The UV/Vis spectra of Au nanoparticles loaded on TiO_2 are shown in Figure 6. The absorbance in the visible region was

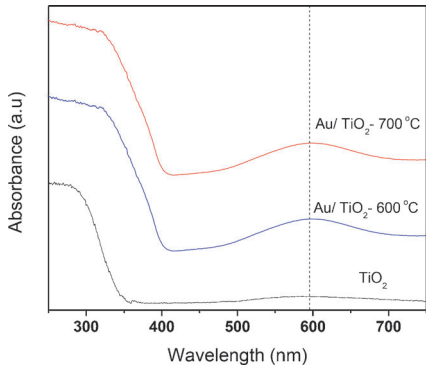

Figure 6. UV/Vis spectra of Au–TiO_2 reduced at different temperatures.

significantly pronounced for the Au/TiO_2 catalyst. The broad absorption peak at 600 nm can be ascribed to the surface plasmon resonance of Au nanoparticles.[14] Although Au had a low refractive index in the visible region, the high refractive index of TiO_2 caused the surface plasmon resonance to shift to a longer wavelength (redshift) from its nominal value of 520 nm in H_2O.[15] The redshift may have been caused by the interaction between Au nanoparticles and the TiO_2 support. The bands shown between 300 and 400 nm are ascribed to TiO_2 in both spectra, which is in agreement with the UV/Vis spectra of Au nanoparticles loaded on the TiO_2 support reported by Loganathan et al.[16]

To obtain information on the chemical states of Au species, X-ray photoemission spectroscopy (XPS) was used; Figure 7 compares the XPS spectra of the Au 4f core level for Au/TiO_2 reduced under a H_2 flow at different temperatures. Each sample demonstrated two peaks owing to Au $4f_{7/2}$ and Au $4f_{5/2}$ transitions. The XPS spectra of the Au 4f core level for all samples were deconvoluted into three pairs of peaks with an Au $4f_{7/2}$ binding energy of (1) 83.7, 84.8, and 86.4 eV for Au^0, $Au^{\delta+}$, and Au^{3+} species, respectively, for the samples reduced at 400 °C; (2) 83.0 and 84.2 eV for Au^0 and $Au^{\delta+}$ species, respectively, for the samples reduced at 600 °C; and (3) 83.0 and 85.9 eV for Au^0 and $Au^{\delta+}$ species, respectively, for the samples reduced at 700 °C.[23] The samples reduced at a low temperature (400 °C) demonstrated the presence of both reduced Au nanoparticles (Au^0) and cationic nanoparticles ($Au^{\delta+}$ and Au^{3+}), which suggests that the reduction at 400 °C cannot completely reduce all Au species to the metallic state. For the samples reduced at 600 and 700 °C, the presence of only Au^0 and $Au^{\delta+}$ oxidation states was observed.

In the case of the Ti 2p photoemission spectra, the XPS peaks of Ti $2p_{3/2}$ and Ti $2p_{1/2}$ binding energies were located at 459.3 and 464.8 eV, respectively, which were indicative of a stoichiometric or defect-free TiO_2 structure for the samples reduced at 400 °C. In the case of Au/TiO_2 samples reduced at 600 °C, the Ti $2p_{3/2}$ peak was located at 458.8 eV, which was indicative of Ti^{3+} whereas the peaks located at 460.1 and 464.9 eV were both indicative of Ti^{4+}. The catalyst sample reduced at 700 °C demonstrated Ti $2p_{3/2}$ peaks at 457.9 and 458.8 eV and Ti $2p_{1/2}$ peaks at 459.7 and 464.5 eV, which indicated that the valence state of Ti in TiO_2 reduced at 700 °C comprised a mixture of Ti^{IV} and Ti^{III}. The Ti 2p peaks located at lower binding energies (457–458.8 eV) were possibly due to the charge transfer by the overlayer Au nanoparticles under the reducing pretreatment conditions and adsorbed OH (or H_2O).[17]

Correlation between the catalyst structure and the catalytic performance

TEM characterization revealed the particle size of 6–8 and 10–12 nm for the catalyst samples reduced at 600 and 700 °C, respectively, but the catalyst samples reduced at 400 °C had a particle size of 4–5 nm. The particle size increased with an increase in reduction temperature owing to the Ostwald ripening effect or particle size agglomeration.[18] However, the cata-

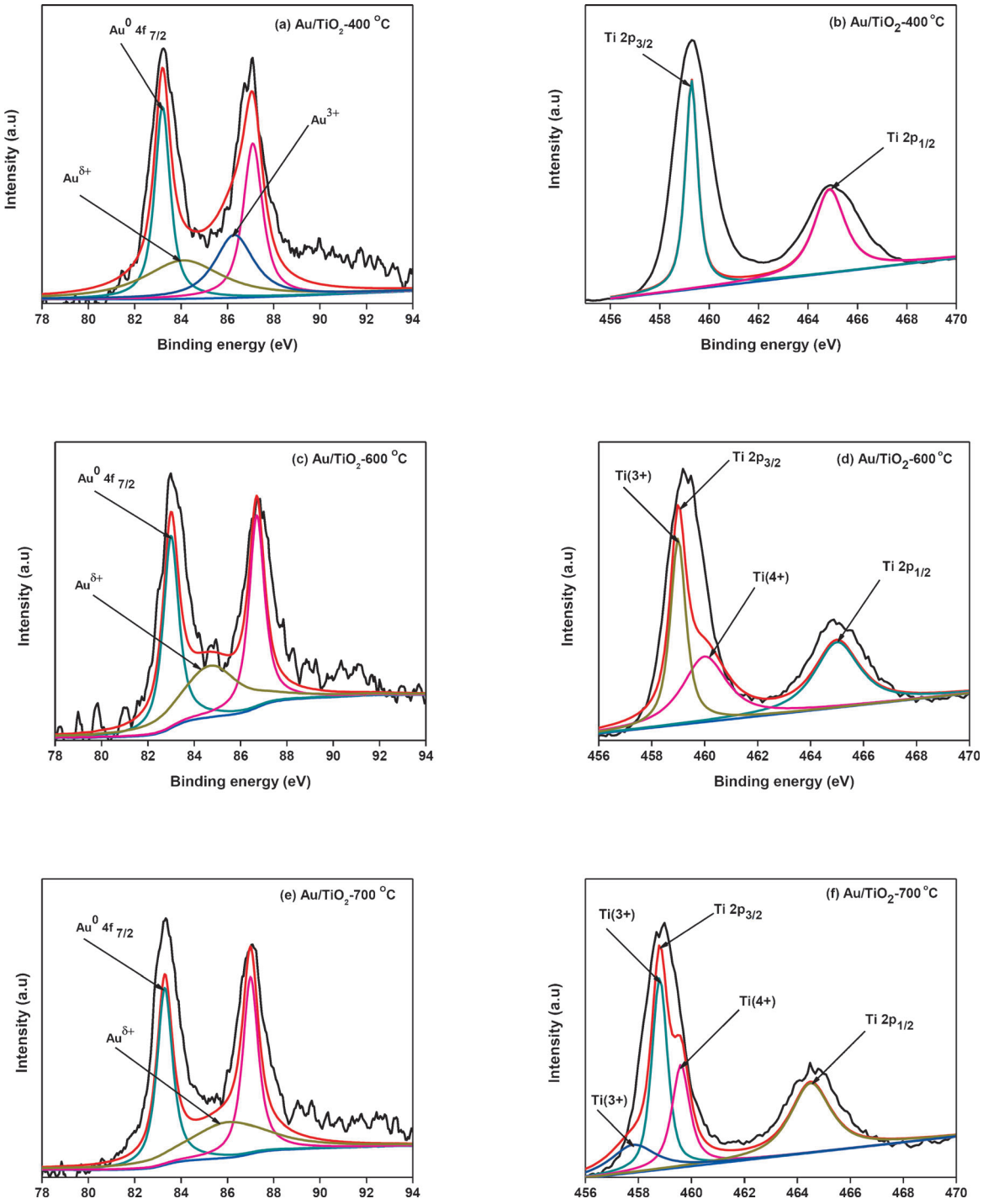

Figure 7. XPS spectra of the Au/TiO_2 samples reduced at different temperatures.

lytic activity for the conversion of cellobiose to gluconic acid increased with an increase in the particle size, which is in contrast to the reports in the literature that emphasized on the effective catalytic activity of Au nanoparticles with size less than 5 nm.[2,3,6–8] This interesting observation indicated that for catalytic oxidation, the activity of supported Au metal nanoparticles as a whole did not solely depend on the size range of metal nanoparticles, but several other factors may also play critical roles in determining the activity.

XPS characterization revealed that the electronic structure of Au significantly changed for the samples reduced at 600 and 700 °C, which was characterized by the shift in the binding energy to a lower value. This shift in binding energy is due to the Schottky junction formed at the metal–oxide support interface. This unique interface enabled electron transfer to occur from the conduction band of the TiO_2 support to the Au metal particles, and this charge may be concentrated on atoms at the interface and the periphery. The particles are thus consid-

ered as "electron-rich," which create O_2 vacancies at oxide surfaces. These O_2 vacancies created at oxide surfaces interacted strongly with the Au nanostructure, which resulted in a significant rearrangement in the electronic structure of Au as well as in covalent bonding between the Au nanoparticles and the defect oxide support. The electrons that are stored in these chemical bonds led to the formation of active Au atoms in the vicinity of the Au–oxide perimeter interface and contributed to the catalytic process by providing an additional adsorption site for the reactant owing to the effective nucleophilic attack of C=O substrate bonds by activated O_2 (O*) at the Au–oxide perimeter interface.[18–28]

Furthermore, critical Au–O–Ti bonds that coupled the Au nanoparticles to the support were expected to be formed in the metal–support interaction. The Au–O bond was polarized to give Au a partial positive charge, and this interaction led to unique dual catalytic active sites for the adsorption and activation of O_2.[29] In an equivalent view of the detailed mechanism of O_2 adsorption and activation, Green et al. reported a back donation of an electron density phenomenon that creates a unique Au–Ti site at the Au/TiO_2 interface, which is critical in the activation of O_2 because this unique Au–Ti site at the perimeter interface of the metal–support interaction allowed for electron transfer from Au to Ti and the subsequent electron transfer to $2\pi^*$ antibonding states of O_2, aiding in O–O bond activation. In addition, the adsorption of O_2 thus occurred via di–σ bonding to Au and Ti to form an Au–O–O–Ti state. The basic O/Au and O/Ti species residing at the perimeter interface of Au–Ti extracted electron density from the substrate and as such readily attacked bound C=O and C=C-containing species and activate C–H and O–H bonds, which thus catalyzed a range of partial and full oxidative reactions.[30]

This hypothesis was supported by DFT studies[28,31–34] that postulated that O_2 dissociation was sensitive to the arrangement of the Au surface atoms and the most active sites for O_2 dissociation are found at the metal–support interface and not at the Au particle surfaces. It was thus reasonable to state that O_2 adsorbed on the edges, at the metal–support interface, and then migrated or diffused to the surfaces of Au particles, and as such, oxidation reactions occurred at the surfaces of Au nanoparticles because of the presence of diffused O*, which could initiate nucleophilic attacks on biomass substrates at the Au particle surfaces, with the subsequent reaction leading to the corresponding gluconic acid. Because theoretical studies reported in the literature have found that the active site for O_2 activation is the perimeter interface between Au nanoparticles and the TiO_2 support, a strong interaction should therefore be indispensable to afford high catalytic activity for cellobiose oxidation.[35]

The increased metal–support interaction that consequently constituted active sites for O_2 adsorption and activation readily reacts with bound hydrocarbon intermediates for the oxidation of C=O bonds contained in most biomass-derived compounds and several carbonyl and aldehyde-containing compounds.[28] Glucose, the main reaction intermediate that was oxidized to yield gluconic acid, contains an aldehyde group (^{1}C), a primary alcohol group (^{6}C), and a secondary alcohol group (^{2}C–^{4}C). The oxidation of the aldehyde group (–CHO) of glucose resulted in the formation of gluconic acid, and the oxidation of both the primary and the secondary alcohol to yield ketones is suppressed if the catalytic system used in the reaction is highly selective and active.

The support properties can tune the interaction with the metal particles deposited on or in it. They can modify both the electronic and structural properties of the catalyst as well as provides different anchoring sites for the reactants, which act as active and sometimes reactive surfaces if strong metal–support interaction effects are induced. Our results and most reports by various researchers show that in addition to acid strength, density and glucan sorption affinity, the textural characteristics of the support and the electronic state of the nanoparticles as a result of electron transfer from the support to the Au nanoparticles during catalyst reductions under a H_2 flow at high temperatures critically determine the catalyst success.

Reaction parameter optimization for cellobiose oxidation

Further kinetic study was performed over the Au/TiO_2 catalyst to gain more insights into the reaction conditions to efficiently convert cellobiose to gluconic acid. The effect of the reaction time on cellobiose conversion and the distribution of oxidative reaction products is shown in Figure 8a. The pressure in the reactor was set at 0.5 MPa. Cellobiose conversion increases with the increase in reaction time. The conversion increases sharply at the initial stage, reaching 93% in 2 h, followed by a gradual increase slowly, and reaching 100% after 12 h. The selectivity of gluconic acid did not follow the same trend. Gluconic acid selectivity is the highest at 2 h and decreases significantly with the increase in reaction time from 2 to 12 h; detailed analysis reveals that gluconic acid further converted to other undesirable products such as lower carbon polyols at a longer reaction time.[34] The best gluconic acid selectivity of 73.7% was obtained at a reaction time of 2 h and an O_2 pressure of 0.5 MPa, which is higher than that reported previously by An et al. (57%) and Wang et al. (63%). The difference can be attributed to the different catalyst preparation method (impregnation) and lower reduction temperature (300 °C) used by them.[8,35]

The effect of O_2 pressure on cellobiose oxidation was studied by varying the pressure from 0.5 to 2.5 MPa at 145 °C (Figure 8b). The conversion of cellobiose was constant regardless of the O_2 pressure. The increase in O_2 pressure affects the distribution of reaction products to a large extent. At an O_2 pressure of 0.5 MPa, a gluconic acid selectivity of 73.7% with an appreciable amount of glycolic acid (25%) was observed. The formation of ethylene glycol and glycolic acid with a subsequent decrease in the selectivity of gluconic acid with the increase in the O_2 pressure from 1.5 to 2.5 MPa indicates that the increase in the amount of dissolved O_2 directly affects the distribution of reaction products. This phenomenon was consistent with the results reported by An et al., in which a decreasing trend in gluconic acid selectivity with an increase in the O_2 pressure from 0.5 to 1.0 MPa was observed, which fa-

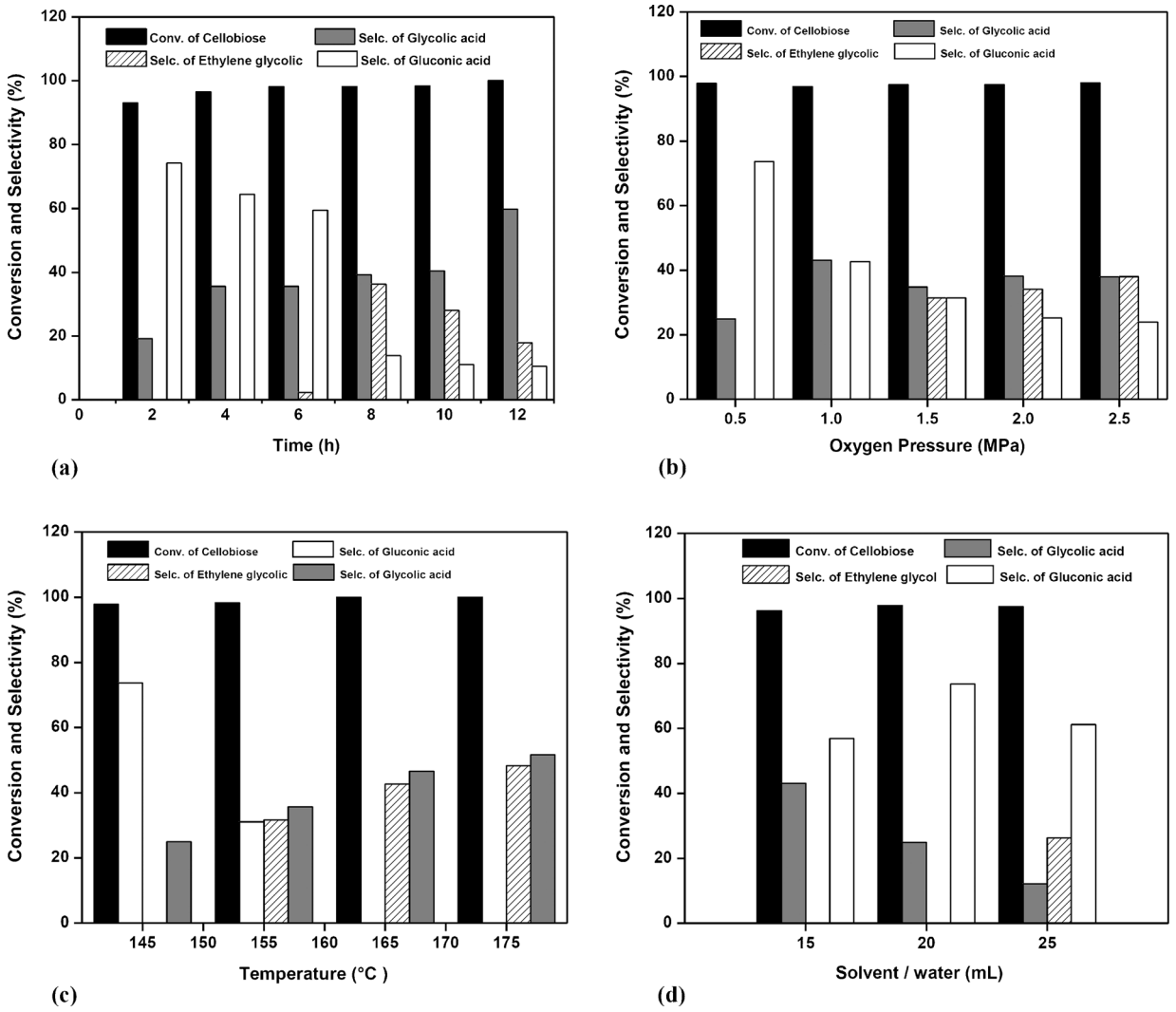

Figure 8. a) Time course for cellobiose conversion over 1 wt% Au/TiO_2 catalyst (reduced at 700 °C) for the selective oxidation of cellobiose. Reaction conditions: 0.050 g of the catalyst, 0.300 mmol of cellobiose, 20 mL of H_2O, $T = 145$ °C, $P = 0.5$ MPa O_2 (other products include fructose and sorbitol). b) Effect of O_2 pressure on the catalytic performance of 1 wt% Au/TiO_2 catalyst (reduced at 700 °C) for the selective oxidation of cellobiose. Reaction conditions: 0.300 mmol of cellobiose, 20 mL of H_2O, 0.050 g of the catalyst, $t = 3$ h (other products include sorbitol and fructose). c) Effect of reaction temperature on the catalytic performance of 1 wt% Au/TiO_2 catalyst (reduced at 700 °C) for the selective oxidation of cellobiose. Reaction conditions: 0.300 mmol of cellobiose, 20 mL of H_2O, 0.050 g of the catalyst, $P = 0.5$ MPa O_2, $t = 3$ h (other products include sorbitol and fructose). d) Effect of solvent amount on the catalytic performance of 1 wt% Au/TiO_2 catalyst (reduced at 700 °C) for the selective oxidation of cellobiose. Reaction conditions: 0.300 mmol of cellobiose, 20 mL of H_2O, 0.050 g of the catalyst, $P = 0.5$ MPa O_2, $t = 3$ h (other products include sorbitol and formic acid).

vored the formation of smaller carbon-containing polyols such as ethylene glycol, acetic acid, and glycolic acid.[8] The optimum O_2 pressure for the oxidation of cellobiose to gluconic acid was observed to be 0.5 MPa.

The effect of the reaction temperature on conversion and selectivity toward gluconic acid is depicted in Figure 8c. The cellobiose conversion increases significantly from 97.86% at 145 °C to 100% at 175 °C at a reaction time of 2 h. The distribution of organic acids changes significantly with temperature. Higher temperatures (150–175 °C) favor the formation of C_2 polyols (ethylene glycol and glycolic acid), which implies that high temperature may cause cellobiose to carbonize and the produced gluconic acid further convert to other undesirable oxidative byproducts.[36] Moreover, high temperature induces a degradation of sugars with fragmentation of the molecules, which results in short-chain carboxylic acids, aldehydes, and so on.[37] Although maximum cellobiose conversion is obtained at a high temperature, gluconic acid selectivity is extremely poor. Considering the energy consumption and the selectivity of the desired product, the optimum reaction temperature was set at 145 °C herein.

To study the effect of the solvent (H_2O) on cellobiose conversion and product distribution, some experiments were performed at varying solvent amounts (Figure 8d). The presence of H_2O favors to a large extent the conversion of cellobiose. Water is essential to promote the hydrolysis reaction of cellobiose to the intermediate glucose. If a different amount of H_2O is added to the reaction system, a substantial increase in the conversion of cellobiose is observed. As the H_2O amount in the reaction system increases from 15 to 20 mL, the conversion

of cellobiose increases from 96.22 to 97.86%; however, as the amount of H_2O increases to 25 mL, the conversion of cellobiose decreases slightly to 97.52%. The selectivity toward gluconic acid increases sharply from 56.86 to 73.72% with the increase in the solvent amount in the reaction system from 15 to 20 mL but decreases dramatically to 61.18% with the increase in the solvent amount to 25 mL. The distribution of the reaction byproducts observed (glycolic acid and ethylene glycol) showed that at 20 mL of the solvent amount, the selectivity toward glycolic acid decreases significantly from 43% (at a solvent amount of 15 mL) to 25%, with no traces of ethylene glycol. As the H_2O amount was increased to 25 mL, an appreciable amount of ethylene glycol and glycolic acid was observed with a selectivity of 26 and 12%, respectively. This result implies that the highest catalytic activity of Au/TiO_2 could be reached at a proper solvent amount.

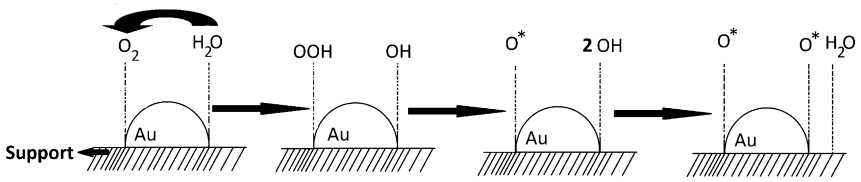

Scheme 1. Plausible activation of O_2 on the active sites of the Au catalyst in the presence of H_2O.

Efforts have been made to understand the nature behind the promotional effect of H_2O on the catalytic activity of Au/TiO_2 in the selective oxidation of cellobiose to gluconic acid. Theoretical studies have shown that the OH groups originating from the dissociation of H_2O could facilitate the O_2 adsorption on TiO_2[38] and the binding and activation of O_2 could be significantly enhanced in the presence of H_2O if O_2 and H_2O are coadsorbed on supported Au nanoclusters.[39] In addition, other studies have revealed that surface H_2O can increase the number of O_2 vacant sites.[40]

From the reaction pathway of our experimental results and some relevant literature information,[41] one can observe that the hydrogen species released from the dissociation of H_2O may readily react with the O_2 adsorbed on the catalyst, which yields the reactive OOH species, which further decompose to form O* species and OH groups. The OH groups would combine first and then dissociate to release O* and H_2O species. The released O* species are highly mobile and would readily react with glucose, which is formed as a result of cellobiose hydrolysis, to form gluconic acid. This finding has confirmed that it is the O* species formed on Au/TiO_2 in the presence of H_2O that help improve the catalytic activity of Au/TiO_2 in the conversion of cellobiose to gluconic acid and also revealed that the presence of an optimum amount of H_2O in the reaction system helps facilitate the O_2 adsorption and activation on the catalyst surface sites. A plausible activation mechanism of O_2 in the presence of H_2O is proposed for the oxidative conversion of cellobiose to gluconic acid over Au/TiO_2 (Scheme 1).

Insights into the reaction pathway

As mentioned earlier, reactions are first performed under the same reaction conditions by using the TiO_2 support without Au nanoparticles and the main reaction product was glucose with a selectivity of 91%. Glucose oxidation under the same reaction conditions was also performed, and Table 1 presents the oxidative conversion of glucose by O_2 in H_2O over Au/TiO_2 catalysts reduced at different temperatures. Product analysis revealed the presence of gluconic acid, glycolic acid, sorbitol, ethylene glycol, and erythritol (a mixture of C_2, C_4, and C_6 carboxylic acids). The formation of sorbitol may be as a result of in situ H_2 produced. Similar reactions were performed with gluconic acid as the reactant, and glycolic acid and ethylene glycol were the major products, which indicated that gluconic acid, which is a C_6 organic acid, is further converted to smaller carbon-containing organic compounds (C_2 organic acids) in the catalytic oxidation of cellobiose to gluconic acids.

Table 1. Oxidative conversion of glucose by O_2 in H_2O over $Au–TiO_2$ catalysts at different reduction temperatures.[a]

Catalyst sample	$T_{reduction}$ [°C]	Cellobiose conversion [%]	Selectivity [%]				
			Gluconic acid	Glycolic acid	Sorbitol	Ethylene glycol	Erythritol
Au/TiO_2[b]	400	100	31.1	32.6	7.5	28.8	0
Au/TiO_2[c]	600	100	46.9	24.2	6.6	22.4	7.3
Au/TiO_2[d]	700	100	67.4	14.3	5.2	13.2	0

[a] Reaction conditions: 0.300 mmol of cellobiose, 20 mL of H_2O, 0.050 g of the catalyst (1 wt% loading), T = 145 °C, P = 0.5 MPa O_2, t = 3 h.

The oxidation of glucose and gluconic acid gives a clearer insight into the reaction pathway, which shows that sorbitol and erythritol (C_6 and C_4 organic compounds, respectively) are formed from glucose whereas glycolic acid and ethylene glycol (both C_2 organic compounds) are formed from the deeper oxidation of gluconic acid. It is also confirmed that a high reduction temperature resulted in better gluconic acid selectivity and less degradation products formed. The proposed mechanism of cellobiose oxidation is shown in Scheme 2.

The hydrolysis occurs via step 1 primarily catalyzed over TiO_2 surfaces, and the major product is glucose. This step is supported by the observation of a small amount of fructose, which is a typical product obtained from glucose through isomerization. Step 2 represents the oxidation step with Au nanoparticles as the active sites, in which glucose is further converted to gluconic acid in the presence of O_2. This step also yields

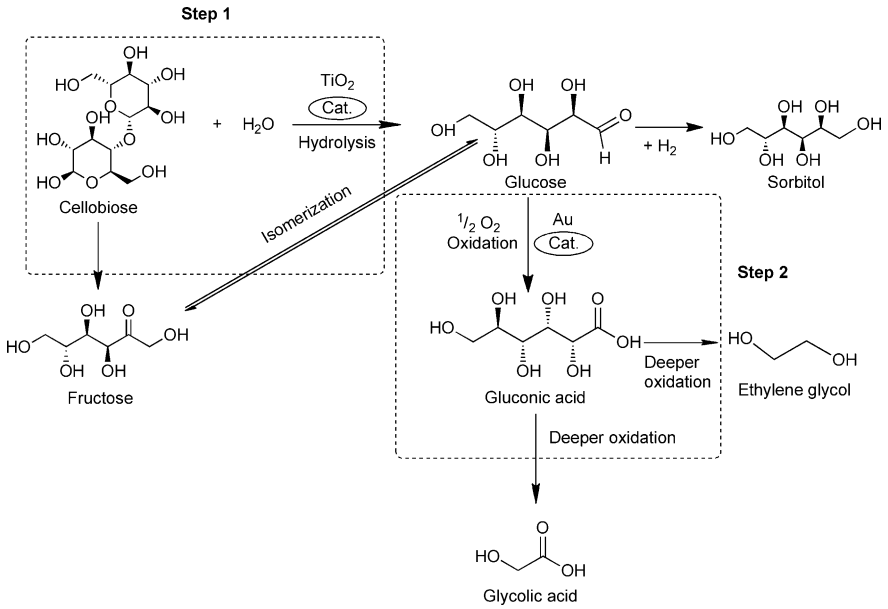

Scheme 2. Possible reaction pathway of the conversion of cellobiose to gluconic acid over the Au/TiO_2 catalyst.

other oxidation products such as ethylene glycol and glycolic acid through further hydrogenolysis of gluconic acid.

Conclusions

The catalytic activity of Au nanoparticles loaded on different supports was investigated, with a focus on the performance to selectively convert cellobiose to gluconic acid. The Au nanoparticles loaded on TiO_2 as a bifunctional catalyst demonstrated superior catalytic activity for the oxidation of cellobiose to gluconic acid in H_2O. The effects of key factors such as the solvent (H_2O) amount, reaction time, reaction temperature, and O_2 pressure on the oxidation of cellobiose were also examined. The experimental results revealed that cellobiose can be converted to gluconic acid with a selectivity higher than 70% if the reaction was catalyzed by Au/TiO_2 at 145 °C and an O_2 pressure of 0.5 MPa within a reaction time of 2 h. The conversion of cellobiose to gluconic acid catalyzed by Au/TiO_2 was observed to be a two-step reaction in which cellobiose was first hydrolyzed to reducing sugar (glucose), which then subsequently oxidized in the presence of O_2 to gluconic acid. In this process, the catalyst support (TiO_2) promoted the conversion of cellobiose to glucose through the hydrolysis reaction whereas Au nanoparticles catalyzed the oxidation of glucose to gluconic acid.

Experimental Section

Catalyst preparation

The Au nanoparticles loaded on TiO_2 were prepared by using the classical deposition–precipitation method. TiO_2 (10 g) was dispersed in deionized (DI) H_2O (400 mL). An appropriate amount of $HAuCl_4$ solution (0.01 M) was added dropwise to this TiO_2 suspension while maintaining the pH at 6.5 by adding NaOH solution (0.1 M). The suspension was thermostated at 70 °C and stirred vigorously for 2 h. After it was cooled to RT, magnesium citrate (0.5 g) dissolved in DI H_2O (100 mL) was added and then the mixture was stirred at RT for 1 h. The catalyst was then filtered, washed with DI H_2O, and dried in an oven at 80 °C. The ground powder was reduced under a H_2 flow at different temperatures for 4 h.

The Au nanoparticles supported on the CNT were prepared by using the method reported by Murphy et al.[9] Briefly, $HAuCl_4 \cdot 3H_2O$ aqueous solution (0.01 M, 0.5 mL) was mixed with $Na_3C_6H_5O_7$ aqueous solution (0.01 M, 0.5 mL) and DI H_2O (18.4 mL). Ice cold, freshly prepared $NaBH_4$ solution (0.1 M, 0.6 mL) was then added to the above mixture under stirring. A measured amount of HNO_3-pretreated CNTs (>95%, Cnano) was added to the as-prepared Au nanoparticle suspension. Ethanol (6 mL) was added immediately under vigorous stirring, and the mixture was ultrasonicated for 10 min. After stirring for an additional 10 h, a black solid was obtained, which was separated through centrifugation, washed with DI H_2O several times, and then dried at 80 °C overnight.

The Au nanoparticles supported on the zeolite HY were prepared by using a coprecipitation method. An appropriate amount of Au precursor ($HAuCl_4$) was dissolved in DI H_2O. Zeolite HY (0.5 g) was added to the aqueous solution, followed by the addition of a sufficient amount of urea predissolved in DI H_2O (30 mL) under vigorous stirring at 80 °C for 6 h. The solid was obtained by filtering and washing with DI H_2O, followed by drying at 60 °C overnight. The ground powder was reduced for 4 h under a H_2 flow (flow rate: 20 mL min^{-1}).

Catalyst characterization

The powder XRD patterns were recorded on a Bruker AXS D8 diffractometer under ambient conditions using CuK_α radiation ($\lambda =$ 0.15406 nm) from a Cu X-ray tube operated at 40 kV and 40 mA. The diffractograms were recorded in the 2θ range of 10–90° (step size: 0.02°), with a count time of 20 s at each point. Before the test, the samples were dried at 80 °C overnight. The TEM images were recorded on JEOL JEM-2100F transmission electron microscope operated at an accelerating voltage of 200 keV. The UV/Vis spectra of the synthesized catalyst were recorded in the scan range of 210–900 nm with a Shimadzu UV-2450 spectrophotometer (Kyoto, Japan) equipped with an integrating sphere and using $BaSO_4$ as a reference.

The EDX analysis (with an EDX-Gatan cyrotransfer system JSM-6700F) and XRF (with a Bruker AXS S4 explorer) analysis were also performed on the sample to confirm the Au loading present. The samples were also analyzed by using XPS. The XPS spectra were recorded on a Thermo ESCALAB 250 spectrometer. The spectra were recorded by using an Al anode (AlK_α radiation at 1486.6 eV) with a 20 eV pass energy (energy step: 0.1 eV) and 0.1 s dwelling time. Energy corrections were performed by using C 1s (284.6 eV) as a reference. NH_3-TPD was performed with a Micromeritics AutoChem II

2920 apparatus. The amount of the catalyst (200 mg) was placed in a quartz U tube, which was heated for 2 h at 600 °C in an Ar atmosphere and then kept at 100 °C for NH_3 adsorption. If the saturated adsorption was achieved, the system was flushed with He for 3 h. Then, the temperature was programmed to increase to 600 °C (heating rate: 10 °C min^{-1}). The desorbed NH_3 was analyzed with a thermal conductivity detector.

Catalytic cellobiose oxidation

The oxidative conversion of cellobiose was performed in a 50 mL Teflon-lined batch reactor (PARR Instrument). Cellobiose (typically 0.300 mmol) and the catalyst (0.050 g) were added to the reactor precharged with DI H_2O. The system was charged with pure O_2 at a controlled pressure after removing air by pressurizing and depressurizing several times with pure O_2. The reaction was performed at different reaction conditions under steady stirring (1200 rpm). After the completion of the reaction, the products were analyzed with a liquid chromatograph equipped with a RID-6A refractive index detector and a Hi-Plex H (300×6.5 mm) column with H_2SO_4 solution (0.01 M) as mobile phase (flow rate: 1 mL min^{-1}).

Acknowledgements

*We acknowledge support from the Ministry of Education Academic Research Fund (AcRF) Tier 2 grant (ARC 5/13), AcRF Tier 1 grant (RG 48/12), and the Singapore Agency for Science, Technology and Research (A*STAR).*

Keywords: bifunctional catalysts · oxidation · gluconic acid · gold · titania

[1] A. Limayem, S. C. Ricke, *Prog. Energy Combust. Sci.* **2012**, *38*, 449 – 467.
[2] B. Kamm, *Angew. Chem. Int. Ed.* **2007**, *46*, 5056 – 5058; *Angew. Chem.* **2007**, *119*, 5146 – 5149.
[3] H. Wang, L. Zhu, S. Peng, F. Peng, H. Yu, J. Yang, *Renewable Energy* **2012**, *37*, 192 – 196.
[4] M. Besson, F. Lahmer, P. Gallezot, P. Fuertes, G. Fleche, *J. Catal.* **1995**, *152*, 116 – 121.
[5] M. J. Climent, A. Corma, S. Iborra, *Green Chem.* **2011**, *13*, 520 – 540.
[6] J. Zhang, X. Liu, M. N. Hedhili, Y. Zhu, Y. Han, *ChemCatChem* **2011**, *3*, 1294 – 1298.
[7] X. Tan, W. Deng, M. Liu, Q. Zhang, Y. Wang, *Chem. Commun.* **2009**, 7179 – 7181.
[8] D. An, A. Ye, W. Deng, Q. Zhang, Y. Wang, *Chem. Eur. J.* **2012**, *18*, 2938 – 2947.
[9] N. R. Jana, L. Gearheart, C. J. Murphy, *Langmuir* **2001**, *17*, 6782 – 6786.
[10] W. Deng, Y. Wang, Q. Zhang, Y. Wang, *Catal. Surv. Asia* **2012**, *16*, 91 – 105.
[11] G. Liang, H. Cheng, W. Li, L. He, Y. Yu, F. Zhao, *Green Chem.* **2012**, *14*, 2146 – 2149.
[12] M. Yang, Y. Men, S. Li, G. Chen, *Appl. Catal. A* **2012**, *433 – 434*, 26 – 34.
[13] S. Tsubota, T. Nakamura, K. Tanaka, M. Haruta, *Catal. Lett.* **1998**, *56*, 131 – 135.
[14] X. Li, T. Fan, H. Zhou, B. Zhu, J. Ding, D. Zhang, *Microporous Mesoporous Mater.* **2008**, *116*, 478 – 484.
[15] S. Chen, Y. Liu, G. Wu, *Nanotechnology* **2005**, *16*, 2360 – 2364.
[16] K. Loganathan, P. Muthaiahpillai, *Environ. Eng. Res.* **2011**, *16*, 81 – 90.
[17] Z. Jiang, W. Zhang, L. Jin, X. Yang, F. Xu, J. Zhu, W. Huang, *J. Phys. Chem. C* **2007**, *111*, 12434 – 12439.
[18] T. W. Hansen, A. T. DeLaRiva, S. R. Challa, A. K. Datye, *Acc. Chem. Res.* **2013**, *46*, 1720 – 1730.
[19] J. Frost, *Nature* **1988**, *334*, 577 – 580.
[20] I. X. Green, W. Tang, M. Neurock, J. T. Yates, *Science* **2011**, *333*, 736 – 739.
[21] J. Plata, A. Márquez, J. Sanz, R. Avellaneda, F. Romero-Sarria, M. Domínguez, M. Centeno, J. Odriozola, *Top. Catal.* **2011**, *54*, 219 – 228.
[22] M. Gao, A. Lyalin, T. Taketsugu, *Catalysts* **2011**, *1*, 18 – 39.
[23] G. Walther, G. Jones, S. Jensen, U. J. Quaade, S. Horch, *Catal. Today* **2009**, *142*, 24 – 29.
[24] P. Buffat, J. P. Borel, *Phys. Rev. A* **1976**, *13*, 2287 – 2298.
[25] D. W. Goodman, *Catal. Lett.* **2005**, *99*, 1 – 4.
[26] J. Radnik, C. Mohr, P. Claus, *Phys. Chem. Chem. Phys.* **2003**, *5*, 172 – 177.
[27] L. Fan, N. Ichikuni, S. Shimazu, T. Uematsu, *Appl. Catal. A* **2003**, *246*, 87 – 95.
[28] S. Laursen, S. Linic, *J. Phys. Chem. C* **2009**, *113*, 6689 – 6693.
[29] G. C. Bond, *Molecules* **2012**, *17*, 1716 – 1743.
[30] I. X. Green, W. Tang, M. Neurock, J. T. Yates, *Acc. Chem. Res.* **2014**, *47* (3), 805 – 815.
[31] A. Villa, G. M. Veith, D. Ferri, A. Weidenkaff, K. A. Perry, S. Campisi, L. Prati, *Catal. Sci. Technol.* **2013**, *3*, 394 – 399.
[32] D. W. Bassett, *Zeolites* **1983**, *3*, 182.
[33] A. Vijay, G. Mills, H. Metiu, *J. Chem. Phys.* **2003**, *118*, 6536 – 6551.
[34] N. Ji, T. Zhang, M. Zheng, A. Wang, H. Wang, X. Wang, Y. Shu, A. L. Stottlemyer, J. G. Chen, *Catal. Today* **2009**, *147*, 77 – 85.
[35] D. An, A. Ye, W. Deng, Q. Zhang, Y. Wang 10th European Congress on Catalysis, EUROPACAT-X, Glasgow, Scotland, August 28 – September 2, 2011.
[36] D. I. Kondarides, X. E. Verykios, *Stud. Surf. Sci. Catal.* **1994**, *82*, 471 – 480.
[37] A. Mirescu, U. Prüße, *Appl. Catal. B* **2007**, *70*, 644 – 652.
[38] L. Liu, B. McAllister, H. Ye, P. Hu, *J. Am. Chem. Soc.* **2006**, *128*, 4017 – 4022.
[39] A. Bongiorno, U. Landman, *Phys. Rev. Lett.* **2005**, *95*, 106102.
[40] O. Pozdnyakova-Tellinger, D. Teschner, J. Kröhnert, F. C. Jentoft, A. Knop-Gericke, R. Schlögl, A. Wootsch, *J. Phys. Chem. C* **2007**, *111*, 5426 – 5431.
[41] X. Yang, X. Wang, C. Liang, W. Su, C. Wang, Z. Feng, C. Li, J. Qiu, *Catal. Commun.* **2008**, *9*, 2278 – 2281.

Received: March 3, 2014
Published online on May 30, 2014